

# IMAGING ADDITIVES ON HUMAN HAIR

## with the PHI *nanoTOF*

### OVERVIEW

A distinct characteristic of time-of-flight secondary ion mass spectrometry (TOF-SIMS) lies in the ability to visualize chemical information in a spatially-resolved manner. There are many instances where TOF-SIMS is utilized to probe the chemistry of fibers (e.g. hair) or of woven and nonwoven materials that are naturally or artificially produced (e.g. wool and polymers). However, more often, it is not the chemistry of the raw product that is under interrogation but, rather, the dispersion of an additive or surfactant on the specimen and its affect on the surface properties. Companies that directly produce or support the cosmetics, petrochemical fibers, textiles and textile care industries often employ TOF-SIMS in product development, or for routine testing (quality control), to glean useful chemical information.

In this Note, we demonstrate the use of the PHI *nanoTOF* to visualize chemical information on a curved surface at high spatial resolution. The interrogated specimen is a human hair that was introduced to the instrument and analyzed in the “as-received” state. The hair was treated before it was submitted for analysis, so both naturally occurring and applied molecules such as 18-methyl eicosanoic acid (18-MEA) and lauryl sulfate, respectively, are observed.

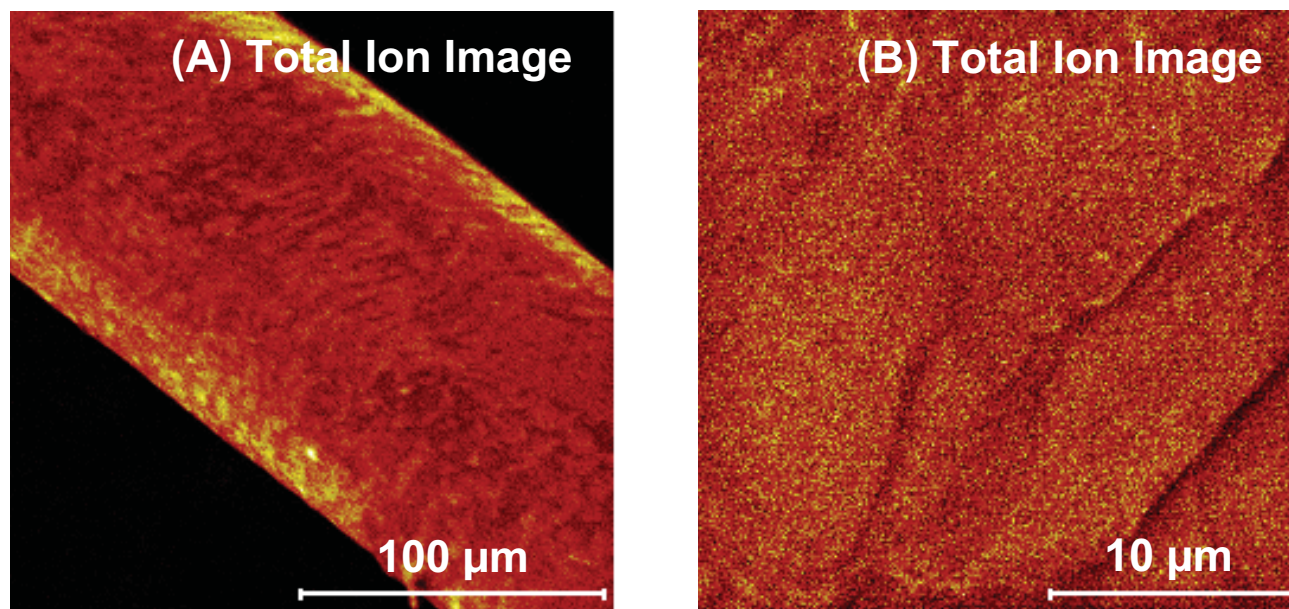


Figure 1: Images of a human hair show the ability of the PHI *nanoTOF* to collect information from the entire curved surface that is visible to the analytical ion beam. Individual cuticles are observable along the hair shaft, and the high magnification image demonstrates the spatial resolution provided by the *nanoTOF*. (A) Total ion image (-SIMS, 200 µm FOV). (B) Total ion image (-SIMS, 25 µm FOV).

A difficulty that is encountered when analyzing a curved insulator is the kinetic energy spread of the secondary ions collected from the probed specimen by the mass spectrometer. The TRIFT analyzer of the PHI *nanoTOF* TOF-SIMS instrument is designed with specific advantages for imaging curved and other topographically rough specimens. In this Note, we explain an important feature of the TRIFT analyzer that allows collection of signal from the entire surface of a curved insulator. The data collected from the human hair specimen is used as a demonstration of this capability.

## EXPERIMENTAL

An unbunched 30 keV Au<sup>+</sup> primary ion beam was used to acquire images of the hair in both the positive and the negative secondary ion polarities. A raw data stream was collected in each secondary ion polarity to allow further post-acquisition evaluation (i.e. retrospective analysis) of the data. Images having large (200 μm x 200 μm) and small (25 μm x 25 μm) fields-of-view were collected operating the Au<sup>+</sup> primary ion beam at DC currents of 0.5 nA and 100 pA, respectively. The raw data streams were collected for 10-15 minutes each, and a digital raster of 256 pixels x 256 pixels was used for each acquisition. Charge neutralization was accomplished using 15 eV electrons.

## RESULTS

Total ion images of the hair are presented in Figure 1. Notice in Figure 1A that numerous submicron-scale cuticles along the shaft of the hair are clearly visible because the hair is probed using a Au<sup>+</sup> beam of small ( $\leq 130$  nm) diameter. A magnified image of the hair surface is given in Figure 1B where the details of the cuticle structures are clearly recognized. In Figure 1A it may also be observed that the secondary ion signal is relatively uniform across the curved sample surface; that is to say, the effects of signal variation as a function surface geometry (topographic contrast) are able to be minimized. This is an important analytical advantage of the TRIFT analyzer because, owing to the uniformity of secondary ion collection, it may be inferred that a difference in the signal intensity as a function of position is indicative of a change in the relative concentration as a function of position.

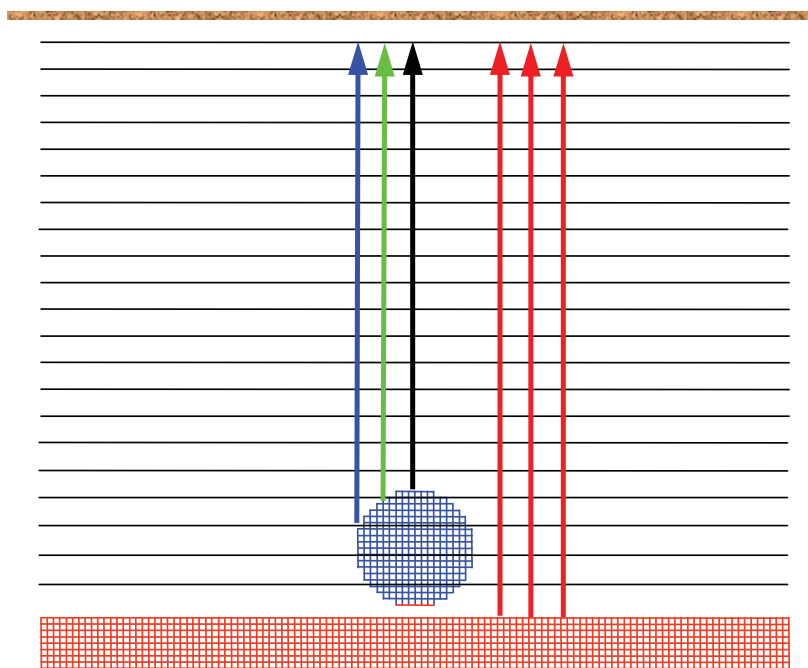


Figure 2: The significance of the TRIFT analyzer's kinetic energy focusing is illustrated in this simulation of the extraction field in the vicinity of a  $\sim 130$  μm particle on a flat substrate (e.g. Si). If, for example, the equipotential lines represent an increment of 45 V, then the kinetic energy difference between ions departing the top (black trace) and the side (blue trace) of the particle is  $\sim 70$  V and between the top of the particle and the substrate (red traces) is  $\sim 195$  V.

The difficulty associated with achieving uniform secondary ion detection across the curved, or topographically rough, surface of an insulating specimen is illustrated in Figure 2. The illustration shows that the extraction field lines penetrate the insulating specimen which is shown sitting on a flat substrate. Secondary ions that depart different points of the probed specimen experience different accelerating potentials before entering the mass analyzer and, therefore, have different kinetic energies. In order to compensate for these topographic effects, an efficient imaging mass analyzer must have the ability to collect ions having a large dispersion in kinetic energy and to compensate for the effect of kinetic energy on the flight times of ions at each mass-to-charge ( $m/z$ ) ratio. The TRIFT mass spectrometer, operating in the standard mode, is able to collect secondary ions with a kinetic energy spread of 240 eV and the embedded triple-ESA focuses the secondary ions in time to compensate for differences in kinetic energy.

Ion specific (chemical) images of the hair specimen are rendered in Figure 3. The images in Figures 3A and 3B show the distributions of  $\text{Ca}^+$  and  $\text{C}_{16}\text{H}_{33}\text{O}_2^+$ , respectively, in the positive secondary ion polarity. The spatial variation of these ion signals is evident and is highlighted in the overlay image presented in Figure 4A. Such observations concerning the spatial variation of chemistry may be made with confidence using the TRIFT mass spectrometer because the effects of topographic shadowing are minimized.

The images in Figures 3C, 3D and 3E show the distributions of an amino acid fragment, a molecular ion of lauryl sulfate, and the molecular ion of 18-MEA in the negative secondary ion polarity. The distributions of the negative polarity ions shown in Figure 3 are very similar indicating that the applied surfactant has been dispersed uniformly across the hair surface. An image overlay at high

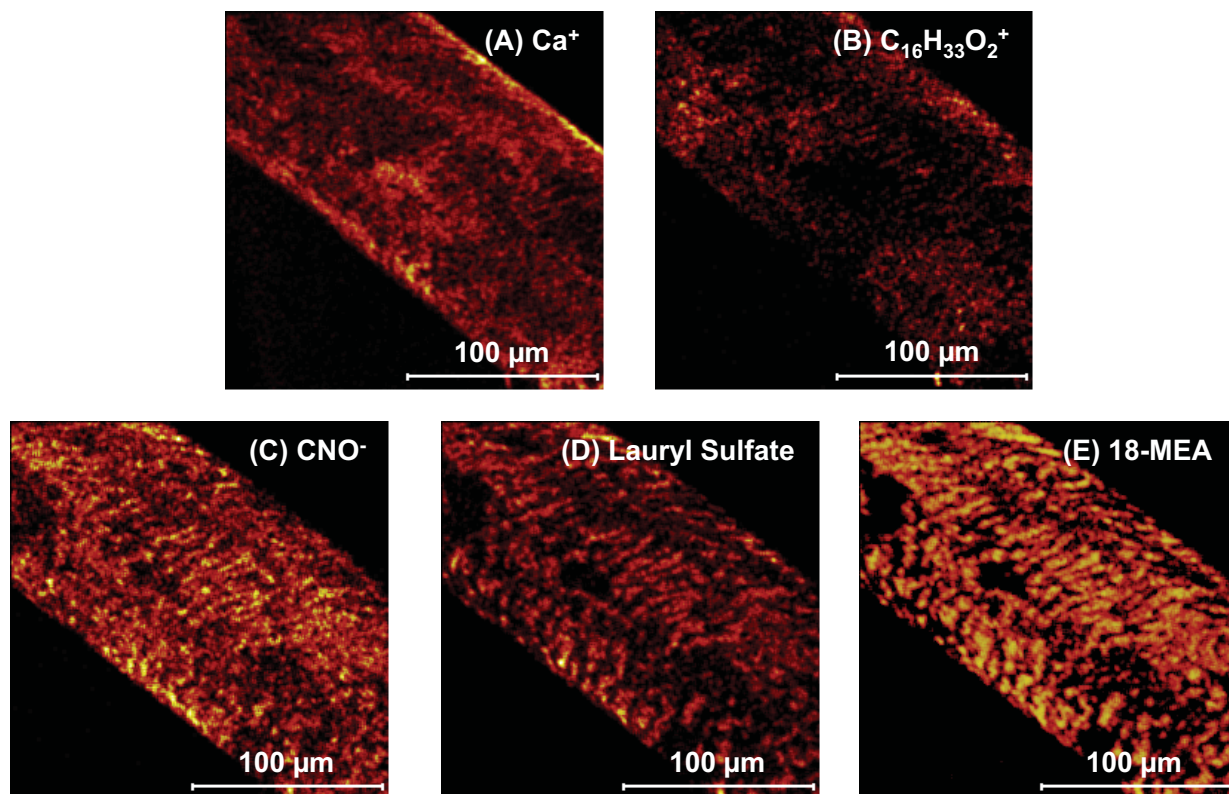


Figure 3: A complete chemical picture of the hair surface is provided by a set of molecule-specific and elemental images. (A) Calcium ( $\text{Ca}^+$ , 40  $m/z$ ). (B) Acid hydrate ( $\text{C}_{16}\text{H}_{33}\text{O}_2^+$ , 257  $m/z$ ). (C) Amino acid ( $\text{CNO}^-$ , 42  $m/z$ ). (D) Lauryl sulfate ( $[\text{M-O}+\text{C}_2\text{H}_4]$ , 293  $m/z$ ). (E) 18-MEA ( $\text{M}$ , 341  $m/z$ ). The field-of-view in each image is 200 µm x 200 µm.

magnification is presented in Figure 4B to show the variation in chemistry with respect to the cuticle structure. The high magnification overlay image is comprised of secondary ion signals from both polarities;  $\text{Na}^+$  (red),  $\text{Ca}^+$  (green) and  $\text{CN}^-$  (blue). The ratio of the  $\text{Ca}^+$  and  $\text{CN}^-$  images emphasizes the considerable anticorrelation in these signals over the analyzed area whereas the ratio of the  $\text{Na}^+$  and  $\text{CN}^-$  images reveals a high degree of correlation. Also notice that the amino acid signal,  $\text{CN}^-$ , is pronounced toward the edge of the cuticles.

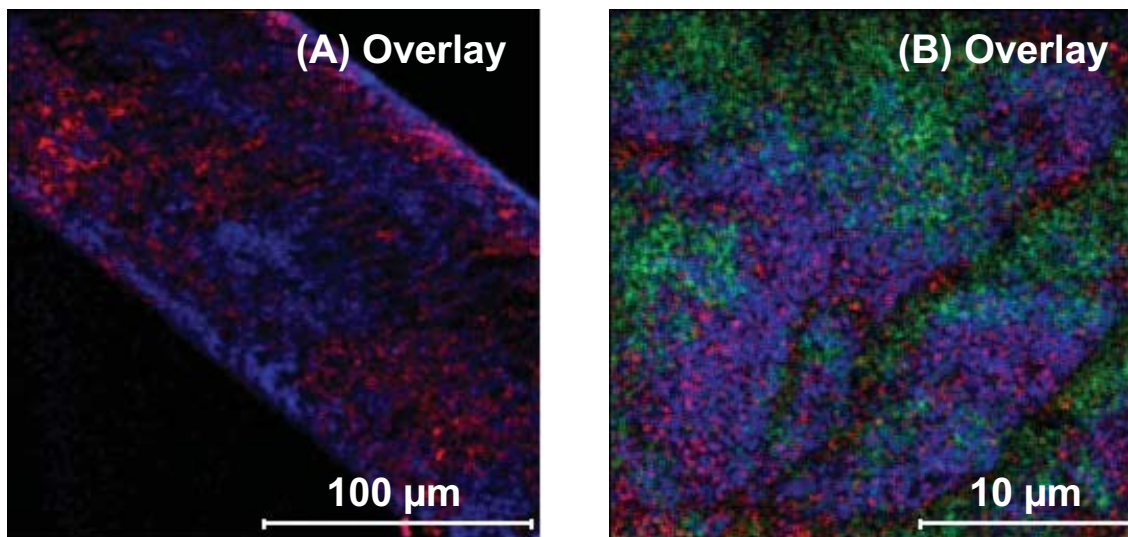


Figure 4: Color overlay images reveal the relative distribution of chemical components on the surface of the hair. (A) 200 μm FOV overlay of  $\text{C}_{16}\text{H}_{33}\text{O}_2^+$  (257 m/z, red) and  $\text{Ca}^+$  (40 m/z, blue). (B) 25 μm FOV overlay of  $\text{Na}^+$  (23 m/z, red),  $\text{Ca}^+$  (40 m/z, green) and  $\text{CN}^-$  (26 m/z, blue).

## CONCLUSION

The PHI *nanoTOF* is unequalled for imaging the lateral distribution of additives and surfactants on topographically rough, insulating specimens; additionally, the probe size of the Au LMIG allows the analyst to resolve small details of the specimen. The kinetic energy focusing characteristics of the TRIFT mass spectrometer were demonstrated by imaging the spatial distribution of both naturally occurring and applied molecular moieties on the curved, insulating surface of a human hair. Observations concerning the spatial variation of chemistry may be made with confidence using the TRIFT mass spectrometer because the effects of topography are minimized.

## ACKNOWLEDGEMENTS & REFERENCES

We would like to thank Dr. Ivan Kempson of the Ian Wark Research Institute at the University of South Australia for providing the hair sample.

**Physical Electronics**  
18725 Lake Drive East,  
Chanhassen, MN 55317  
952-828-6200  
www.phi.com

**ULVAC-PHI, Inc.**  
370 Enzo, Chigasaki, Kanagawa,  
253-8522, Japan  
81-467-85-4220  
www.ulvac-phi.co.jp



**PHYSICAL  
ELECTRONICS**